

Dynamics of shear-driven droplets on a plane

Didier Bresch¹, Nicolas Cellier², Fred Couderc³, Marguerite Gisclon¹, Pascal Noble³, Gael Richard⁴, Christian Ruyer-Quil²
and Jean-Paul Vila³

¹LAMA Laboratoire de Mathématiques, Université Savoie Mont Blanc, Chambéry, France

²LOCIE Laboratoire d'Optimisation de la Conception et Ingénierie de l'Environnement,
Université Savoie Mont Blanc, Chambéry, France

³IMT Institut de Mathématiques de Toulouse, Toulouse, France

⁴Univ. Grenoble Alpes, INRAE, ETNA, Grenoble, France

June 2022

Augmented skew-symmetric system for thin film flows

Most of the material of this presentation is published in :

Augmented skew-symmetric system for shallow-water system with surface tension allowing large gradient of density.

D.Bresch, N. Cellier, F. Couderc, M. Gisclon, P. Noble, G. Richard, C. Ruyer-Quil, J.-P. Vila. *J. Comp. Phys.* **419** (2020) 109670.

This work has been supported by the Fraise project, grant ANR-16-CE06-0011 of the French National Research Agency (ANR) and by the project Optiwind, Horizon 2020/Clean Sky2 (call H2020-CS2-CFP06-2017-01) with Saint-Gobain. This work was granted access to the HPC resources of CALMIP supercomputing center under the allocation 2019-P1234.



Motivation

- inclusion of surface tension in thin-film equations leads to a third-order operator which limits numerical implementation (cartesian grid and time-step limitation)
- limitation to linearised formulation ($\|\nabla h\| \ll 1$)
- need to account for full curvature in case of contact lines with large contact angles, e.g. movement of a water drop on a metallic surface



Framework

- Euler-Lagrange formalism of Shallow-Water equations

$$\begin{cases} \partial_t h + \operatorname{div}(h\mathbf{u}) = 0 \\ \partial_t(h\mathbf{u}) + \operatorname{div}(h\mathbf{u} \otimes \mathbf{u}) + \nabla P = -\operatorname{div}(\nabla h \otimes \nabla_{\mathbf{p}} E) + \nabla(h\operatorname{div}(\nabla_{\mathbf{p}} E)) \end{cases}$$

- with h the fluid height, \mathbf{u} the fluid velocity vector field and $\mathbf{p} = \nabla h$.
- internal energy E

$$E(h, \nabla h) = \Phi(h) + \sigma(h)\mathcal{E}_{\text{cap}}(\|\nabla h\|)$$

- pressure P

$$\begin{aligned} P(h, \nabla h) &= h\partial_h E(h, \nabla h) - E(h, \nabla h) \\ &= \pi(h) - (\sigma(h) - h\sigma'(h))\mathcal{E}_{\text{cap}}(|\nabla h|) \end{aligned}$$

and

$$\frac{\pi(h)}{h^2} = \left(\frac{\Phi(s)}{s} \right)'|_{s=h}$$

Shallow-Water equations with surface tension

- internal energy E

$$E(h, \nabla h) = \frac{1}{2} g_z h^2 + \frac{\sigma}{\rho} \sqrt{1 + \|\nabla h\|^2}$$

- pressure P is given by

$$P(h, \nabla h) = \frac{1}{2} g_z h^2$$

Idea

- introduce an additional variable \mathbf{v} such that:

$$\frac{1}{2}h\|\mathbf{v}\|^2 = \frac{\sigma}{\rho}(\sqrt{1 + \|\nabla h\|^2} - 1)$$

- surface energy is written as a kinetic energy so that the free energy E reads

$$E(h, \nabla h) = \frac{1}{2}g_z h^2 + \frac{\sigma}{\rho}(\sqrt{1 + \|\nabla h\|^2} - 1) = \frac{1}{2}g_z h^2 + \frac{1}{2}h\|\mathbf{v}\|^2$$

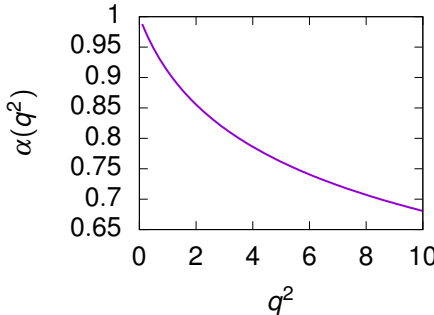
- If $\|\nabla h\| \ll 1$ then $E(h, \nabla h) \approx \frac{1}{2}g_z h^2 + \frac{\sigma}{\rho} \|\nabla h\|^2$ (linearized surface tension)

- \mathbf{v} is related to $\mathbf{p} = \nabla h$ by

$$\mathbf{v} = \alpha(q^2) \mathbf{p} \sqrt{\frac{\sigma}{\rho} \frac{1}{h}}, \quad \text{with} \quad \alpha(q^2) = \frac{\sqrt{2(\sqrt{1+q^2}-1)}}{q}$$

where $q = \|\mathbf{p}\| = \sqrt{\mathbf{p}^t \mathbf{p}}$

- this relation defines unequivocally the additional velocity \mathbf{v}



Construction of evolution equation for $h\mathbf{v}$:

- $h\mathbf{v} = \alpha(q^2) \sqrt{\sigma(h)} h^{3/2} \frac{\nabla h}{h} = \alpha(q^2) G(h) \mathbf{a}$ with $\mathbf{a} = \nabla(\log h)$
- manipulation of the mass balance to get evolution equations for \mathbf{p} , αq^2 , $G(h)$ and \mathbf{a}
- $\nabla \{ h^{-1} [\partial_t h + \mathbf{u} \cdot \nabla h + h \operatorname{div}(\mathbf{u})] \} = 0$ gives
$$\partial_t \mathbf{a} + \nabla(\mathbf{u}^t \mathbf{a}) + \nabla(\operatorname{div}(\mathbf{u})) = 0$$
- $G'(h) [\partial_t h + \mathbf{u} \cdot \nabla h + h \operatorname{div}(\mathbf{u})] = 0$ gives
$$\partial_t G(h) + \mathbf{u}^t \nabla G(h) = -h G'(h) \operatorname{div}(\mathbf{u}),$$

and so on ... The capillary terms in the momentum balance

$-\operatorname{div}(\nabla h \otimes \nabla_{\mathbf{p}} \sigma \mathcal{E}_{\text{cap}}) + \nabla(h \operatorname{div}(\nabla_{\mathbf{p}} \sigma \mathcal{E}_{\text{cap}}))$ are next rewritten to achieve a skew-symmetric formulation.

Skew-symmetric augmented formulation

We thus obtain:

$$\partial_t \mathbf{U} + \operatorname{div}(\mathcal{F}(\mathbf{U})) = \mathcal{M}.$$

où

$$\begin{aligned}\mathbf{U} &= \begin{pmatrix} h \\ h\mathbf{u} \\ h\mathbf{v} \end{pmatrix}, \quad \mathcal{F}(\mathbf{U}) = \begin{pmatrix} h\mathbf{u} \\ h\mathbf{u} \otimes \mathbf{u} + g_z \frac{h^2}{2} I_d \\ h\mathbf{v} \otimes \mathbf{u} \end{pmatrix} \\ \mathcal{M} &= \begin{pmatrix} 0 \\ \operatorname{div}(h\nabla(f(h, \mathbf{v})\mathbf{v})^t) - \nabla(g(h, \mathbf{v})^t\mathbf{v}) \\ -f(h, \mathbf{v})\operatorname{div}(h\nabla\mathbf{u}^t) - g(h, \mathbf{v})\operatorname{div}\mathbf{u} \end{pmatrix}.\end{aligned}$$

\mathcal{M} is skew-symmetric.

surface tension terms are generalized diffusion terms !

where $f(h, \mathbf{v})$ is a symmetrical tensor and $g(h, \mathbf{v})$ is a vector defined as

$$f(h, \mathbf{v}) = \left(\sqrt{\frac{\sigma}{\rho}} \frac{\sqrt{h}}{\sqrt{1 + \frac{\rho h}{4\sigma} \|\mathbf{v}\|^2}} \right) \left(\mathbf{I} - \left(1 + \frac{\rho h}{2\sigma} \|\mathbf{v}\|^2 \right)^{-1} \frac{\rho h}{4\sigma} \mathbf{v} \otimes \mathbf{v} \right)$$

$$g(h, \mathbf{v}) = \frac{h\mathbf{v}}{2} \left(1 + \frac{\rho h}{2\sigma} \|\mathbf{v}\|^2 \right)^{-1}.$$

- If (h, \mathbf{u}) is regular enough and if the IC \mathbf{v}_0 verifies $\mathbf{v}_0 = \alpha(\|\nabla h_0\|^2) \sqrt{\frac{\sigma}{\rho} \frac{1}{h_0}} \nabla h_0$ holds, then \mathbf{v} corresponds to $\mathbf{p} = \nabla h$ and (h, \mathbf{u}) is solution to shallow-water equation with surface tension.

Energy balance

- energy

$$\begin{aligned} E_{tot} &= \frac{\|h\mathbf{u}\|^2}{2h} + E(h, \mathbf{p}) \\ &= \frac{\|h\mathbf{u}\|^2}{2h} + g_z \frac{h^2}{2} + \frac{\|h\mathbf{v}\|^2}{2h} \end{aligned}$$

- entropic variables

$$(\nabla_U E_{tot})^t = V^t = \left(-\frac{1}{2} \left(\|\mathbf{u}\|^2 + \|\mathbf{v}\|^2 \right) + g_z h, \mathbf{u}^t, \mathbf{v}^t \right).$$

- $V^t \{\partial_t U + \operatorname{div}(F(U))\} = V^t \mathcal{M}$ gives

$$\begin{aligned} \partial_t E_{tot} + \operatorname{div}(\mathbf{u}(E_{tot} + \pi(h))) &= V^t \mathcal{M} \\ &+ \operatorname{div} [h\mathbf{u}^t \nabla^t (f(h, \mathbf{v})^t \mathbf{v}) - h \nabla \mathbf{u} f(h, \mathbf{v}) \mathbf{v}] \\ &- \operatorname{div} [\mathbf{u} g(h, \mathbf{v})^t \mathbf{v}] \end{aligned}$$

energy is conserved !

IMplicit-EXplicit scheme

- explicit step (hyperbolic part)

$$\frac{U^{n+1/2} - U^n}{\Delta t} + \operatorname{div}(F(U^n)) = 0$$

- semi-implicit step (surface energy part)

$$\frac{U^{n+1} - U^{n+1/2}}{\Delta t} = \mathcal{M}^{n+1}$$

with \mathcal{M}^{n+1} given by:

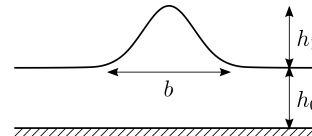
$$\begin{pmatrix} 0 \\ \operatorname{div}(h^{n+1} \nabla(f(h^{n+1}, \mathbf{v}^{n+1/2}) \mathbf{v}^{n+1})^t) - \nabla(g(h^{n+1}, \mathbf{v}^{n+1/2})^t \mathbf{v}^{n+1}) \\ -f(h^{n+1}, \mathbf{v}^{n+1/2}) \operatorname{div}(h^{n+1} \nabla(\mathbf{u}^{n+1})^t) - g(h^{n+1}, \mathbf{v}^{n+1/2}) \operatorname{div} \mathbf{u}^n \end{pmatrix}$$

linear system for \mathbf{v}^{n+1}

- numerical shceme is entropy stable under classical CFL condition

$$\max_K \frac{\Delta t}{m_K} m_e \|\nabla_{\mathbf{U}} F(\mathbf{U}_K^n)\| < a < 1$$

Numerical test (1D)



gaussian disturbance on a water layer at rest:

Augmented
formulation

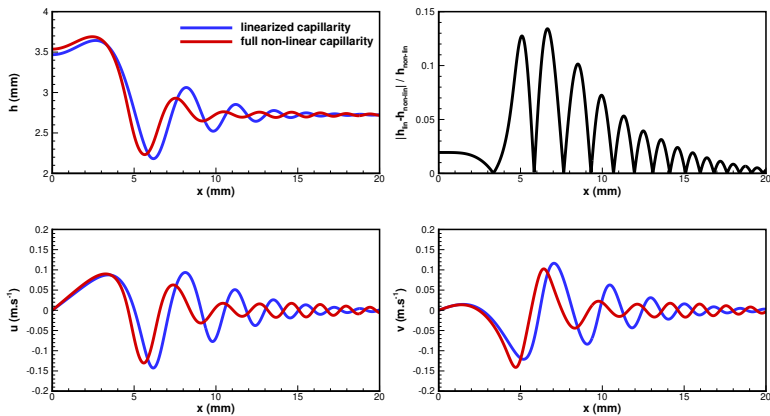
Numerical test

Falling film

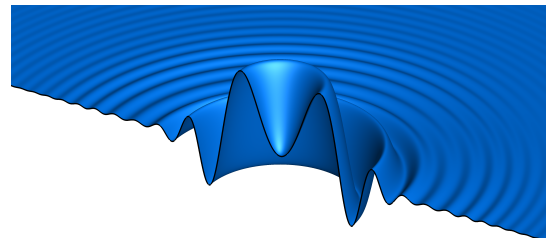
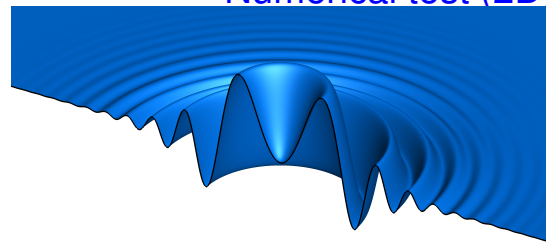
Drop simulation

Single drops

Drops and rivulets



Numerical test (2D)



3200×3200 cells. Top: full ST ; Bottom: linearized ST

Falling film on an inclined plane

Augmented
formulation

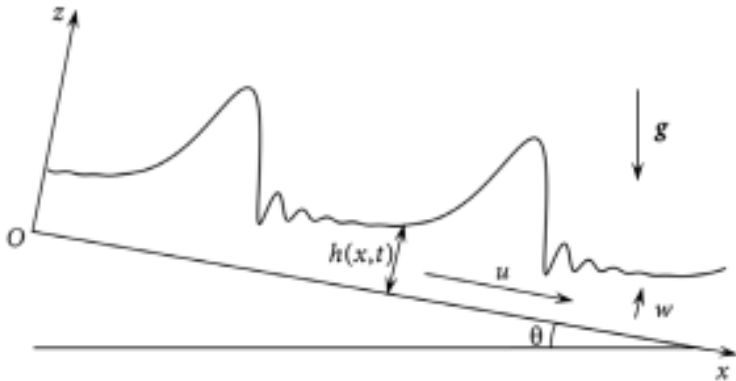
Numerical test

Falling film

Drop simulation

Single drops

Drops and rivulets



- model derived by G. Richard et al.¹

$$\partial_t h + \partial_x (hu) = 0,$$

$$\begin{aligned} \partial_t (hu) + \partial_x \left(hu^2 + \frac{2}{225} \lambda^2 h^5 + \frac{h^2 \cos \theta}{2 \text{Fr}^2} \right) = \\ \frac{1}{\text{Re}} \left(\lambda h - \frac{3u}{h} \right) + \frac{9}{2 \text{Re}} \partial_x (h \partial_x u) + \frac{1}{\text{We}} h \partial_x \mathcal{K}. \end{aligned}$$

where \mathcal{K} is the curvature, equal to $\partial_{xx} h$ (linearized case) or $\partial_x \left(\partial_x h / \sqrt{1 + \partial_x h^2} \right)$ (full curvature case)

$$\text{Re} = h_N u_N / v = gh_N^3 \sin \theta / (3v^2), \quad \text{Fr} = u_N / \sqrt{gh_N},$$

$$\text{We} = \rho h_N u_N^2 / \sigma, \quad \lambda = \text{Resin} \theta / \text{Fr}^2 = 3$$

¹G.L. Richard, M. Gisclon, C. Ruyer-Quil, J.-P. Vila, Optimization of consistent two-equation models for thin flows, Eur. J. Mech. B, Fluids **76** (2019) 725.

- augmented formulation

$$\partial_t h + \partial_x (hu) = 0,$$

$$\partial_t (hu) + \partial_x \left(hu^2 + \frac{2}{225} \lambda^2 h^5 + \frac{h^2 \cos \theta}{2 \text{Fr}^2} \right) =$$

$$\frac{1}{\text{Re}} \left(\lambda h - \frac{3u}{h} \right) + \frac{9}{2\text{Re}} \partial_x (h \partial_x u)$$

$$+ \partial_x [h \partial_x (f(h, v)v)] - \partial_x (g(h, v)v)$$

$$\partial_t (hv) + \partial_x (huv) = -f(h, v) \partial_x (h \partial_x u) - g(h, v) \partial_x u$$

- linearized curvature

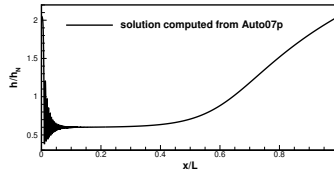
$$f(h, v) = \sqrt{\frac{h}{\text{We}}} \quad \text{and} \quad g(h, v) = \frac{hv}{2}$$

- full curvature

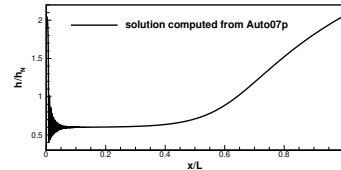
$$f(h, v) = \sqrt{\frac{h}{\text{We}}} \frac{\sqrt{1 + \frac{h\text{We}}{4} v^2}}{1 + \frac{h\text{We}}{2} v^2}, \quad g(h, v) = \frac{hv}{2} \left(1 + \frac{h\text{We}}{2} v^2 \right)^{-1}$$

Traveling Wave solutions

- TW solution of augmented formulation constructed by time-dependent simulations with periodic BCs. Comparisons to TW solutions to the initial formulation (with AUTO07p software²
- vertical wall, $Re = 80$, $Ka = 1000$, $L = 400h_N$, $v = 0.9310^6 \text{ m}^2\text{s}^{-1}$,
 $\rho = 994.3 \text{ kg m}^{-3}$, $\sigma = 19.3 \text{ mN/m}$.

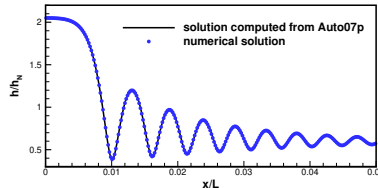


linearized surface tension

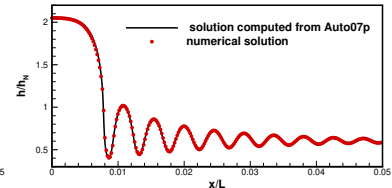


full surface tension

²E.J. Doedel, T.F. Fairgrieve, B. Sandstede, A.R. Champneys, Y.A. Kuznetsov, X. Wang, AUTO-07P: continuation and bifurcation software for ordinary differential equations, Technical report, 2007.



linearized surface tension



full surface tension

Excellent convergence of the augmented numerical formulation to the initial one is observed.

Consistent model of sliding droplets

$$\frac{\partial h}{\partial t} + \operatorname{div}(h \mathbf{U}) = 0,$$

$$\begin{aligned} \frac{\partial h \mathbf{U}}{\partial t} + \operatorname{div}\left(h \mathbf{U} \otimes \mathbf{U} + h^3 \Phi\right) &= \frac{3}{R_e} \left(\frac{\tau_e}{2} - \frac{\mathbf{U}}{h} \right) + h \operatorname{grad} \Pi(h) \\ &\quad + \operatorname{div}(h \nabla f(h, \mathbf{W}) \mathbf{W}^t) - \nabla(g(h, \mathbf{W})^t \mathbf{W}). \end{aligned}$$

$$\frac{\partial h \mathbf{W}}{\partial t} + \operatorname{div}(h \mathbf{W} \otimes \mathbf{U}) = -f(h, \mathbf{W}) \operatorname{div}(h \nabla \mathbf{U}^t) - g(h, \mathbf{W}) \operatorname{div} \mathbf{U},$$

$$\begin{aligned} \frac{\partial h \Phi}{\partial t} + \operatorname{div}(h \Phi \otimes \mathbf{U}) - 2h(\operatorname{div} \mathbf{U}) \Phi + \operatorname{grad} \mathbf{U} \cdot h \Phi + h \Phi \cdot (\operatorname{grad} \mathbf{U})^T \\ = -\frac{1}{Re} \frac{\beta}{h} \left[\Phi - \frac{\mathbf{U} \otimes \mathbf{U}}{3h^2} + \frac{1}{12h^2} \left(\mathbf{U} \otimes \mathbf{U} - \frac{h^2}{4} \tau_e \otimes \tau_e \right) \right] \end{aligned}$$

where

$$f(h, \mathbf{W}) = \sqrt{\kappa} \sqrt{h} \left(1 + \frac{h}{4\kappa} \|\mathbf{W}\|^2 \right)^{-1/2} \left(\mathbf{I} - \frac{h}{4\kappa} (1 + \frac{h}{2\kappa} \|\mathbf{W}\|^2)^{-1} \mathbf{W} \otimes \mathbf{W} \right)$$

$$g(h, \mathbf{W}) = \frac{h\mathbf{W}}{2} \left(1 + \frac{h}{2\kappa} \|\mathbf{W}\|^2 \right)^{-1}$$

Energy balance

$$\text{energy } E_{\text{tot}} = h\mathbf{e} = \frac{1}{2}h||\mathbf{U}||^2 + \frac{1}{2}h||\mathbf{W}||^2 + E_d(h)$$

$$\begin{aligned} \frac{\partial h\mathbf{e}}{\partial t} + \operatorname{div} \left(h\mathbf{e}\mathbf{U} + h^3\varphi \cdot \mathbf{U} - (h\Pi_d + E_d)\mathbf{U} \right) &= \left[\frac{3}{\varepsilon Re} \left(\frac{\tau_e}{2} - \frac{\mathbf{U}}{h} \right) \right] \cdot \mathbf{U} \\ &\quad - \frac{1}{\varepsilon Re} \frac{\beta h}{2} \left(\operatorname{tr}\varphi - \frac{\mathbf{U} \cdot \mathbf{U}}{4h^2} - \frac{\tau_e \cdot \tau_e}{48} \right) \\ &+ \operatorname{div} \left[h\mathbf{U}^t \nabla^t (f(h, \mathbf{W})^t \mathbf{W}) \right] - \operatorname{div} [h\nabla \mathbf{U} f(h, \mathbf{W}) \mathbf{W}] \\ &\quad - \operatorname{div} [\mathbf{U} g(h, \mathbf{W})^t \mathbf{W}] \end{aligned}$$

where E_d is the disjoining energy and $\Pi_d(h) = -\partial_h E_d$ is the disjoining pressure.

Partial wetting

- regularization of wetting properties ($\sigma_{lg} \neq \sigma_{sl}$) with disjunction energy E_d
- Derjaguin formulation

$$\begin{aligned} E_d(h) &= \frac{(n-1)(m-1)}{n-m} \kappa [\cos(\theta_s) - 1] \\ &\quad \times \left[\frac{1}{1-n} \left(\frac{h^*}{h} \right)^{n-1} - \frac{1}{1-m} \left(\frac{h^*}{h} \right)^{m-1} \right] \end{aligned}$$

- pression de disjonction

$$\begin{aligned} \Pi_d(h) &= -\partial_h E_d \\ &= \frac{(n-1)(m-1)}{n-m} \frac{\kappa [1 - \cos(\theta_s)]}{h^*} \left[\left(\frac{h^*}{h} \right)^n - \left(\frac{h^*}{h} \right)^m \right] \end{aligned}$$

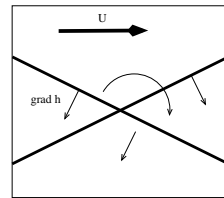
with $(m, n) = (3, 4)$

Introducing disjoining pressure is a regularization of energy jump from κ to $\kappa \cos(\theta_s)$ at contact line:

- $\Pi_d(h^*) = 0$
- $\Pi_d(h) > 0$ for $h < h^*$ and $\Pi_d(h) < 0$ for $h > h^*$ thus $h = h^*$ is stable
- $E_d(h^*) = \kappa[\cos(\theta) - 1]$ and $E_d = 0$ for $h \gg h^*$
- E_d varies continuously from $E_d(h^*) \approx 0$ to $E_d(h^*) = \kappa[\cos(\theta) - 1]$ thus Young-Dupré relation is verified if solid substrate moved to $h = h^*$

Hysteresis of static contact angle

- advancing contact angle $\theta_a \neq$ receding contact angle θ_r
- orientation of the contact line: front if $\mathbf{U} \cdot \nabla h < 0$, rear instead leads to spurious numerical oscillations and failures

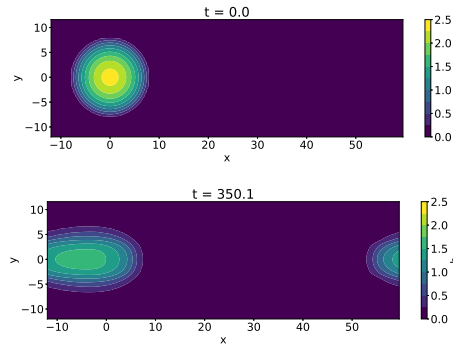


- orientation of contact line based on $\operatorname{div}(h\mathbf{U}) = -\partial_t h$
- jump regularization

$$\theta_s = \frac{\theta_a + \theta_r}{2} + \frac{\theta_r - \theta_a}{2} \tanh(\operatorname{div}(h\mathbf{U})/\varepsilon)$$

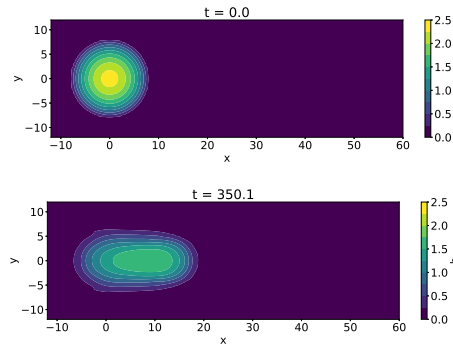
Single sliding drops

No hysteresis

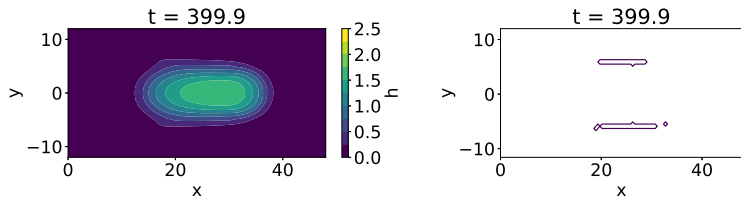


Snapshot of the free surface elevation at the end of a simulation of a drop (initial radius $R_{\text{theta}} = 0.8$ mm) in a domain of size $2.4 \text{ mm} \times 7.2 \text{ mm}$ with $N \times 3N = 1.08 \times 10^4$ nodes for a constant contact angle $\theta_s = 30^\circ$.

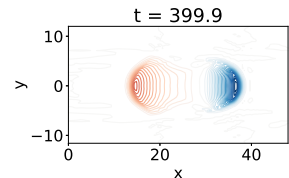
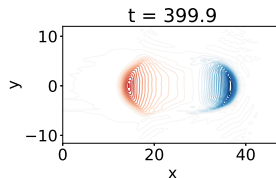
with hysteresis



Snapshot of the free surface elevation at the end of a simulation of a drop (initial radius $R_\theta = 0.8 \text{ mm}$) in a domain of size $2.4 \text{ mm} \times 7.2 \text{ mm}$ with $N \times 3N = 1.08 \times 10^4$ nodes for $2\delta\theta_s = 10^\circ$ ($\theta_a = 35^\circ$ and $\theta_r = 25^\circ$).

elevation h

locations where $1.2h^* < h < 2h^*$ and $|\operatorname{div}(hU)| < \varepsilon$
hysteresis $2\delta\theta_s = 10^\circ$ ($\theta_a = 35^\circ$ and $\theta_r = 25^\circ$).

 $\operatorname{div}(hU)$ $U \cdot \operatorname{grad} h$

hysteresis $2\delta\theta_s = 10^\circ$ ($\theta_a = 35^\circ$ and $\theta_r = 25^\circ$).

Augmented
formulation

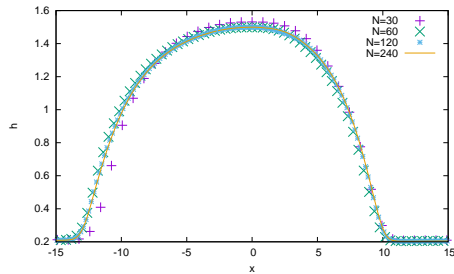
Numerical test

Falling film

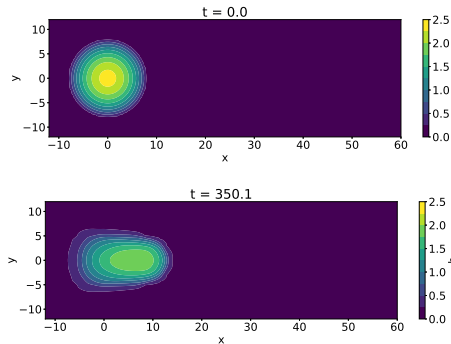
Drop simulation

Single drops

Drops and rivulets



Convergence test. $L = 24$, contact angle $\theta_s = 30^\circ$
 $\delta/h^* = 2$ for $N = 60$.



Snapshot of the free surface elevation at the end of a simulation of a drop (initial radius $R_{\text{theta}} = 0.8$ mm) in a domain of size $2.4 \text{ mm} \times 7.2 \text{ mm}$ with $N \times 3N = 1.08 \times 10^4$ nodes for $2\delta\theta_s = 18^\circ$ ($\theta_a = 39^\circ$ and $\theta_r = 21^\circ$).

Augmented
formulation

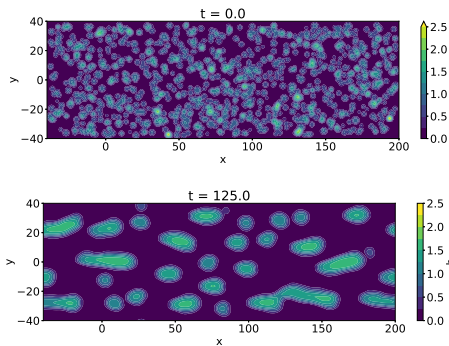
Numerical test

Falling film

Drop simulation

Single drops

Drops and rivulets



Simulation of drop accumulations in a domain of size $8 \text{ mm} \times 24 \text{ mm}$ with $N \times 3N = 3 \times 10^4$ nodes ($N = 100$) for a constant contact angle $\theta_s = 30^\circ$.

Augmented formulation

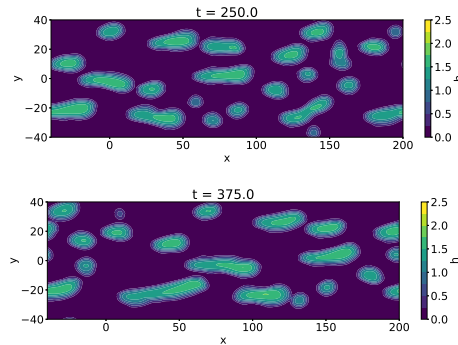
Numerical test

Falling film

Drop simulation

Single drops

Drops and rivulets



Augmented formulation

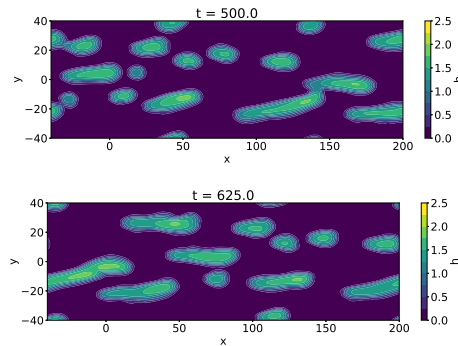
Numerical test

Falling film

Drop simulation

Single drops

Drops and rivulets



Augmented formulation

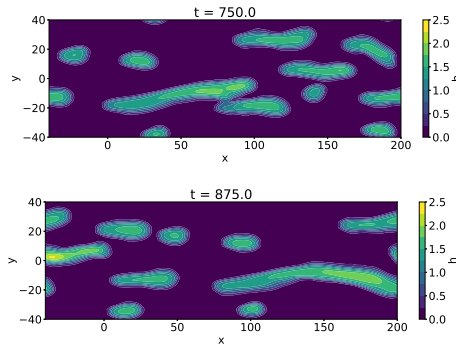
Numerical test

Falling film

Drop simulation

Single drops

Drops and rivulets



Augmented
formulation

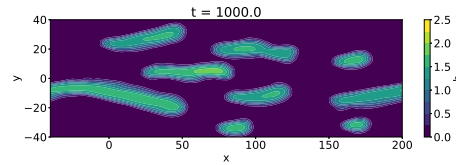
Numerical test

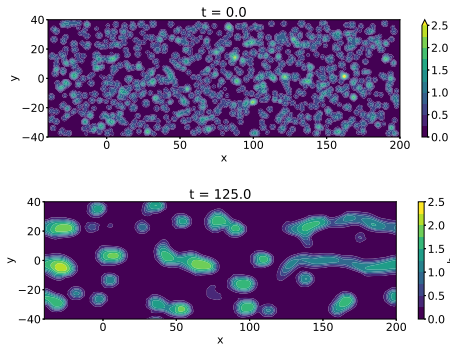
Falling film

Drop simulation

Single drops

Drops and rivulets





Simulation of drop accumulations in a domain of size $8 \text{ mm} \times 24 \text{ mm}$ with $N \times 3N = 3 \times 10^4$ nodes ($N = 100$ and $\delta = 80 \mu\text{m}$) for $2\delta\theta_s = 10^\circ$ ($\theta_a = 35^\circ$ and $\theta_r = 25^\circ$). Initial condition: 1000 droplets of volume 4.4 mm^3 with mean radius $80 \mu\text{m}$.

Augmented formulation

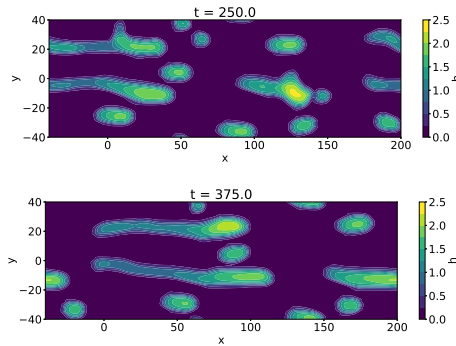
Numerical test

Falling film

Drop simulation

Single drops

Drops and rivulets



Augmented
formulation

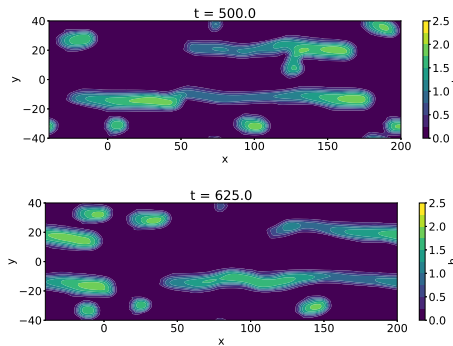
Numerical test

Falling film

Drop simulation

Single drops

Drops and rivulets



Augmented formulation

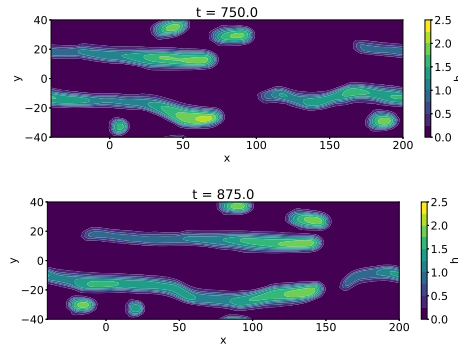
Numerical test

Falling film

Drop simulation

Single drops

Drops and rivulets



Augmented formulation

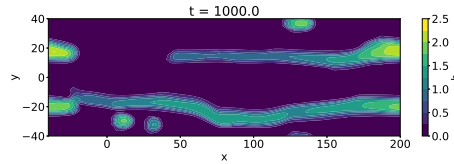
Numerical test

Falling film

Drop simulation

Single drops

Drops and rivulets



Augmented
formulation

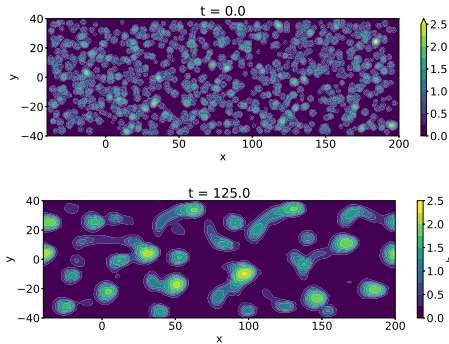
Numerical test

Falling film

Drop simulation

Single drops

Drops and rivulets



Simulation of drop accumulations in a domain of size $8 \text{ mm} \times 24 \text{ mm}$ with $N \times 3N = 3 \times 10^4$ nodes ($N = 100$) for $2\delta\theta_s = 14^\circ$ ($\theta_a = 37^\circ$ and $\theta_r = 23^\circ$).

Augmented formulation

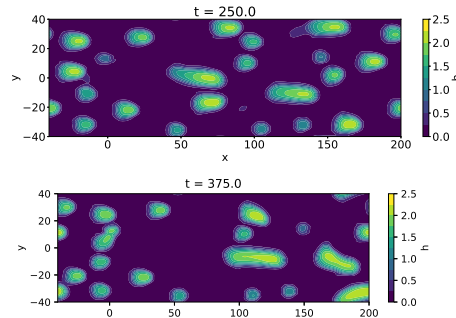
Numerical test

Falling film

Drop simulation

Single drops

Drops and rivulets



Augmented formulation

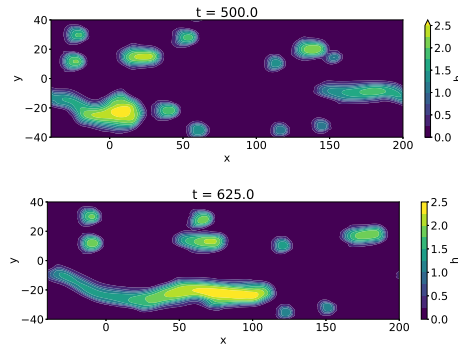
Numerical test

Falling film

Drop simulation

Single drops

Drops and rivulets



Augmented formulation

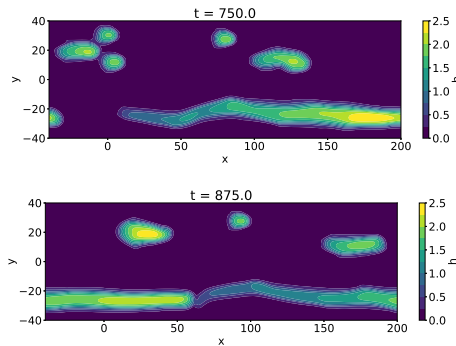
Numerical test

Falling film

Drop simulation

Single drops

Drops and rivulets



Augmented formulation

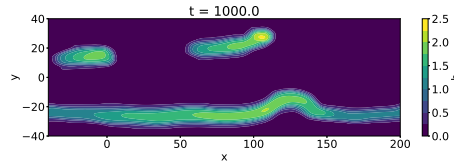
Numerical test

Falling film

Drop simulation

Single drops

Drops and rivulets



Conclusion

- augmented formulation enables to exchange 3rd order surface tension terms into 2nd order diffusion-like terms (appropriate for irregular grids)
- conservation of capillary energy is guaranteed by the augmented formulation
- efficient IMEX scheme with CFL condition
- consistent modelling of sheared liquid films accounting for contact angle hysteresis
- elongation and slowdown of single drops due to hysteresis of contact angle